

# THE STUDY OF BREAKDOWN VOLTAGES FOR TRIGGERED SPARK GAP SWITCHES

*H. Golnabi*

*Institute of Water and Energy  
Sharif University of Technology  
Tehran, Iran*

**Abstract** This study explains the breakdown mechanism in different triggered spark gap switches. Two different trigger electrode configurations are tested for the switch predischage operation in a nitrogen laser circuit. The behavior of the breakdown voltage, when a trigger pulse is applied to the trigger electrode, is investigated, and the results are reported. Based on the experimental measurements new empirical expressions for breakdown voltages are obtained. The self triggered breakdown voltage is also calculated and the differences between the self triggered and external triggered breakdown voltages are reported.

**Key Words** Spark Gap, Breakdown Voltage, Electrical Discharge, Uniform Field Electrode, Laser Triggering

**چکیده** در این مقاله ویژگی های شکست الکتریکی گاز و میزان ولتاژ مورد نیاز برای کلید جرقه مدار لیزر بحث و بررسی شده است. ولتاژ شکست الکتریکی دو نوع از کلید جرقه ای سه الکترودی ساخته شده اندازه گیری شده و نتایج حاصل با ولتاژ شکست حالت دو الکترودی مقایسه شده است. با استفاده از نتایج به دست آمده روابط جدیدی برای محاسبه ولتاژ شکست این کلیدها ارائه شده است که رفتار آنها را از نظر ولتاژ شکست بر حسب فشار گاز و فاصله الکترودها به خوبی نشان می دهد. مطالعات انجام شده نشان می دهد که تخلیه الکتریکی برای کلید جرقه ای سه الکترودی که الکترود سوم در میان کاتد آن قرار داشته یکنواخت تر بوده است که این پدیده عملاً در کاربرد آن در مدار لیزر ازت مشاهده شده است.

## INTRODUCTION

For voltages higher than 10 kV, no solid state electronic element is capable of operating as a reliable switch. Different types of thyratrons can switch high voltages and currents with time delay of about 10  $\mu$ s and very low jitter down to a few nanoseconds. However these elements are expensive and the application is aggravated by the energy supply required for heating the cathode [1]. Thus, for high voltage engineering only spark gaps are nearly unlimited in applications [2] - [8], if they are properly controlled [9]. Spark gaps are now used extensively in the field of high voltage engineering, plasma research, and laser physics to switch electrical energy at high voltages and currents [10].

Design and construction of spark gaps require essential information about the electrical breakdown in gases, ionization and deionization processes, electrode processes, discharge mechanism, and the transition state from self-sustained discharge to a complete breakdown. Also, some knowledge about the breakdown conditions in uniform and non-uniform fields are required. The sparking and minimum breakdown voltages are the points that are to be taken into consideration in the gas breakdown mechanism [11].

In the early stage of the gas breakdown, the corona by trigger electrode, and the cathode electrons are the prime source for the gas ionization. However, several other processes such as photoionization, and thermal ionization must be taken into account. In addition,

different ion loss mechanisms such as deionization by recombination, negative ion formation, and diffusion should also be considered in analysis.

### GAS BREAKDOWN MECHANISMS

If the process of electron multiplication by electron collision, ionization by secondary electron and electron loss by attachment are considered simultaneously in a gas, then neglecting other processes the expression for the current becomes [12, 13]:

$$I = I_0 [\exp(\alpha - \eta)d - (\eta/\alpha)] / \{(\alpha - \eta) - \alpha\gamma[\exp(\alpha - \eta)d - 1]\} \quad (1)$$

where  $I_0$  is the current generated by primary electrons of the cathode, and  $d$  is the distance from cathode to anode. Parameters  $\alpha$  and  $\gamma$  are the Townsend's primary and secondary ionization coefficient, respectively, and  $\eta$  is the electron attachment coefficient.

In two-electrode gaps, cathode plays a very important role in gas discharge and this in switch operation. This electrode supplies the initial electrons for the ionization initiation, for sustaining and for the completion of the discharge. There are several ways in which the required energy may be supplied to release the electrons. These include (1) photoelectronic emission, (2) electron emission by positive ions and excited atom impact, (3) thermionic emission, (4) field emission, and (5) secondary electron emission by photon impact [13]-[14].

The process of transition from self-sustained discharges to breakdown is explained first by the Townsend mechanism. As the voltage between electrodes in a gas increases, the electrode current increases in accordance with Equation 1. At some point, there is a sudden transition from the dark current  $I_0$  to a self-sustaining discharge. At this point the current  $I$  becomes indeterminate as the denominator in the Equation 1 vanishes. This condition

can be shown as:

$$\alpha\gamma[\exp(\alpha - \eta)d] / (\alpha - \eta) = 1 \quad (2)$$

since  $\alpha \gg \eta$  approximately, then,

$$\gamma[\exp(\tilde{\alpha}d) - 1] = 1 \quad (3)$$

where  $\tilde{\alpha}$  represents the effective ionization coefficient.

Theoretically the value of the current at this stage becomes infinitely large, but in practice it is limited by the external circuitry and some other processes. Equation 3 defines the condition for onset of spark and is called the Townsend criterion for spark formation or Townsend breakdown criterion. In this situation, the discharge is then self-sustaining and can continue in the absence of the source producing  $I_0$ . So, this criterion can be said to define the sparking threshold in Townsend gas breakdown mechanism.

An alternative expression is obtained by rewriting Equation 3 as:

$$\tilde{\alpha}d = \ln(1 + 1/\gamma) = K \quad (4)$$

where  $\tilde{\alpha}$  is often very strongly dependent upon gas pressure or field strength. The exact value of  $K$  is of minor importance and can be treated as a constant for many conditions of  $p$  and  $E$ . However, the growth of the charge carrier in a uniform field described by Townsend exponential rate is valid only as long as the electrical field of the space charges of electrons and ions can be neglected compared with the external field.

When the charge concentration is higher than  $10^6$  but lower than  $10^8$ , the growth of an avalanche is weakened, and if the carrier number in avalanche reaches  $10^8$ , the space charge field becomes the same magnitude as the applied field. Under this condition, the space charge developed in an avalanche is ca-

pable of transforming the avalanche into channels of ionization known as a "streamer", that leads to rapid development of breakdown.

### III. Gap Breakdown Voltage

The breakdown voltage of the gap can be determined by the Townsend criterion Equation 3 and by the use of appropriate  $\tilde{\alpha}/p$  and  $\gamma$  corresponding to the low value of  $E/P$ . For the currents below  $10^{-7}$  A, the spark charge distortions are kept to minimum, and more importantly, no damage to electrodes is observed. If  $\tilde{\alpha}/p = f(E/P)$  is used in the Equation 3 we obtain:

$$f(E/P) pd - \ln(1 + 1/\gamma) = K \quad (5)$$

For uniform field  $V_b = Ed$ , where  $V_b$  is the breakdown voltage, then Equation 5 becomes:

$$\exp[f(V_b/d) pd] = K \quad (6)$$

or

$$V_b = f(pd) \quad (7)$$

which means that the breakdown voltage of a uniform field gap is a unique function of the product of pressure and electrode separation for a particular gas and electrode material. Equation 7 is known as the Paschen's law, and has been established experimentally.

The breakdown voltage for the uniform field gaps in air over a wide range of pressure and gap length is given by Schumann [13]:

$$\tilde{\alpha}/p = C [(E/p) - (E/p)_c]^2 \quad (8)$$

Where  $C$  is a constant and  $E_c$  is the limiting value of  $E$  at which effective ionization starts. Combining this relation with the criterion Equation 4 the breakdown voltage becomes:

$$V_b = (K/C)^{1/2} (Pd)^{1/2} + (E/P)_c (pd) \quad (9)$$

Inserting the constants  $E_c$  and  $K/C$ , Equation 9 becomes:

$$V_b = 6.72 (Pd)^{1/2} + 24.36 (pd) \quad \text{kV} \quad (10)$$

which is valid for uniform field gaps in the air for a range of the product  $pd$  from  $10^{-2}$  bar-cm ( $10^{-8}$  pa-m) to  $5 \times 10^2$  bar-cm ( $5 \times 10^4$  pa-m).

In non-uniform fields, such as point-plane, and sphere-plane gaps, the field strength and, thus, the ionization coefficient can vary across the gap. In this case, the electron multiplication is governed by the integral of  $\alpha$ , over the defined path, i.e.:

$$\tilde{\alpha} = \int \alpha dx \quad (11)$$

The criterion condition here, for breakdown may be determined by modifying the discussed formulation for the uniform field to take into account the non-uniform distribution of  $\alpha$ .

In a uniform field gap, when the criterion is satisfied, the ionization process usually leads to a complete breakdown of the gap. But, in non-uniform fields, various discharge processes known as "corona" are observed long before the complete breakdown occurs. These processes may be transient or in a steady state depending on the nature of field gap. In most cases, where there is a non-uniform field, the phenomenon of corona discharge is of particular importance.

### SPARK GAP DESIGNS

The field distorted spark gap switches are developed here, because of their simplicity and because they could be designed with electrodes of large area. On triggering, large amounts of ionization are known to be produced all along the edge of the trigger electrode, and it is hoped that this would result in the circuit carrying arcs on successive discharges being distributed over this large area. This yields a small rate of erosion

per unit area of electrodes, and as a result would increase the switch lifetime.

Our spark gaps are basically three-electrode switches, consisting of a high voltage electrode, a low voltage electrode, and a trigger electrode mounted in a proper place inside the discharge region. Details of the design and construction of these switches are reported recently [15].

Two kinds of controlling mechanisms for the spark gap condition are employed. In the first design, the gap electrode distance, and in the second one, the gas pressure is varied during the measurements. In both mechanisms, however, the critical product ( $pd$ ) can be controlled precisely. Atmospheric operation of the electrode-controlled spark gap is also possible, which is demonstrated in this work.

Figure 1 shows a simplified diagram of the two designed spark gaps. The first design, as shown in Figure 1a, is constructed of two adjustable plane electrodes with a grid held between them as the trigger electrode. While the distance between the main electrodes can be adjusted, with respect to each other, their distances can also be varied with respect to the grid. The diagram of the second gap is presented in Figure 1b, which is a three electrode system consisting of a high voltage electrode, a low-voltage electrode, and a trigger assembly mounted inside the

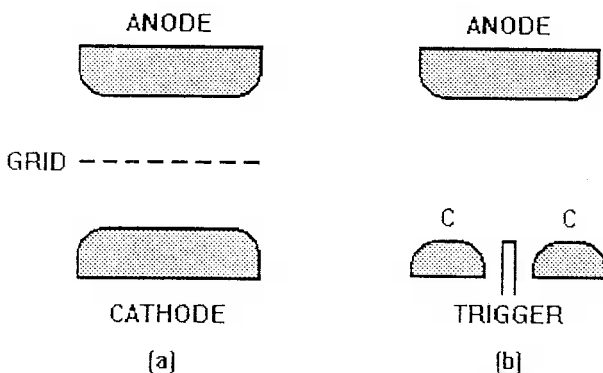


**Figure 1.** A simple diagram for the spark gaps. (a) the grid trigger electrode and (b) the pin trigger electrode configuration for the designed spark gaps.

grounded low-voltage electrode.

In order to test the constructed spark gaps, a Blumlein-driven nitrogen laser is used in which the two switches can be examined as the trigger element. A simple circuit is used for generating a high voltage pulse of about 5 kV to trigger the spark gaps.

## RESULTS AND DISCUSSIONS

### A. Gap Distance-controlled Sprak Gap

To study the breakdown voltage variation, the main gap distance is changed from 4 mm to 20 mm and the breakdown voltages are measured. Figure 2 shows the measured values of these voltages,  $V_b$ , while the distance between the mesh electrode and the cathode is 2mm. For measuring this voltage, it is confirmed that the switch is not self firing at this voltage level. For measuring the breadkdown voltages, the nitrogen gas pressure in the laser tube is high enough that the breakdown can not occur in the laser main discharge tube.

In this experiment, the atmospheric air pressure is considered for the spark gap operation and analysis.

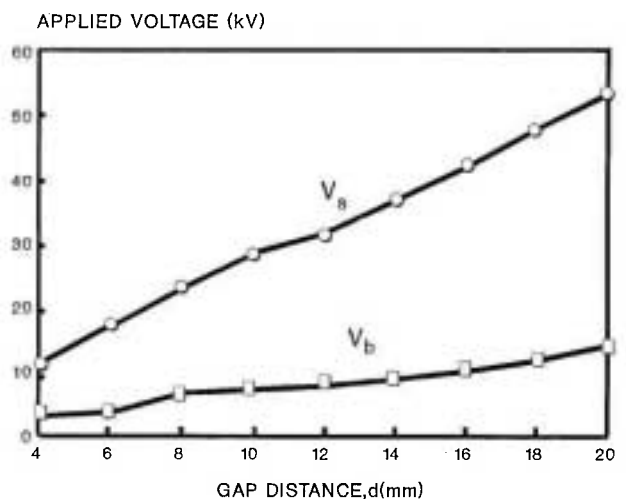


**Figure 2.** The measured average breakdown voltage,  $V_b$ , as a function of the main gap distance,  $d$ , for the grid triggered gap. The self breakdown voltage,  $V_s$ , is calculated from Equation 10.

The self triggered breakdown voltages,  $V_s$ , calculated from Equation 10, is also displayed in Figure 2. The breakdown voltage,  $V_b$ , which shows the effectiveness of the field distroction by the mesh electrode in the discharge process.

In the second measurement the role of the trigger electrode distance, i.e., mesh electrode, with respect to the cathode (ground) electrode is investigated. For this purpose this parameter is changed from 1 mm to 4mm, and the spark gap operation and its voltage breakdown are studied. The observation shows that the optimum distance for the system is in the range of 2-3 mm, Therefore, the breakdown voltages for these values are investigated. The results of these measurements for the two values of  $d_1$  are presented in Figure 3.

It is noticed that this parameter has a major effect on the stable operation of this spark gap and, as a result, on the laser system. As shown in Figure 3, at higher mesh distance, the threshold breakdown voltage increases with distance at first, but at some higher distances, the voltage relatively decreases for the same main gap vvalue. The operational main gap distance for this switch is 17 mm at applied voltage of 13 kV, where the mesh distance is about 2mm with

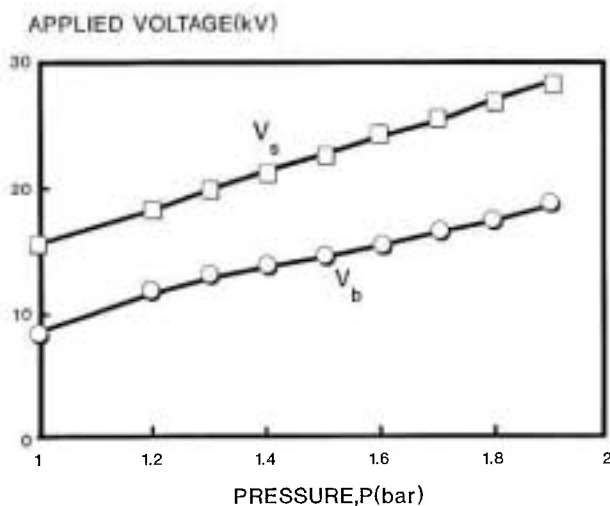


**Figure 3.** The behavior of the breakdown voltage as a function of the grid distance from the cathode,  $d_1$ .

the trigger pulse of 5 kV.

### B. Pressure-controlled Spark Gap

To investigate the breakdown voltage for this switch, this parameter is measured in a similar way that was described in the previous section. The main gap distance in this case is constant of about 5 mm and the annular distance between the trigger electrode and the cathode is fixed at about 1.5 mm. By connecting the outlet of the spark gap to a sensitive gauge and a needle valve, the smooth variation of nitrogen gas pressure in the switch is accomplished. The gas pressure is changed from 1 bar ( $1 \times 10^4$  pa) to 2 bar ( $2 \times 10^4$  pa) at gauge in 0.1 bar ( $1 \times 10^5$  pa) step, and as described above the switch breakdown voltages are measured.

The voltage behavior for this spark gap as a function of the gap pressure is shown in Figure 4, where as the same trigger pulse of about 5 kV is applied to the trigger electrode. Using the given values for  $pd$  product in Equation 10, the self triggered breakdown voltage is calculated which is also displayed in Figure 4. The comparison between the two voltages indicated that the breakdown voltage,

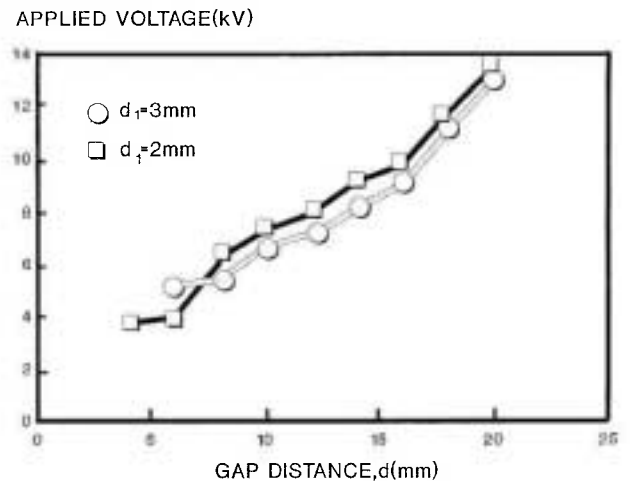


**Figure 4.** The measured average breakdown voltage,  $V_b$ , of the pin triggered gap as a function of the nitrogen gas pressure. Self breakdown voltage,  $V_s$ , is also shown.

$V_b$ , is considerably lower than the self triggering voltage,  $V_s$ , which shows that the field distortion produced by the third electrode considerably reduces the breakdown voltage for the gap. There is, therefore, a good margin between the laser operating voltage and the spark gap breakdown voltage.

### C. Comparison of the two Spark Gaps

There are basically two phases to closing a spark gap. The first is the initial phase of streamer formation at the high electric field region surrounding the trigger electrode and its propagation to the opposite electrode. This is followed immediately by the second phase of arc formation which switches on the electrical breakdown. The time lags (delay) associated with the first and second phases are known as statistical and formation time, respectively. In practice, most of the timing jitter is known to be related to the first process.

For the triggered spark gaps, it is noticed that the placement of the trigger electrode inside the discharge has a major effect on the field distortion and the initial phase of ion formation. The pin electrode mounted in the cathode electrode (Figure 1b) provides a more uniform breakdown field than the mesh electrode assembly of Figure 1a. The reason is that the initial phase of ionization is just in the small region surrounding the trigger pin electrode, and then it propagates from cathode to anode in a more uniform fashion. The first phase of streamer formation is, therefore, limited to a small area which results in a nearly uniform field for the second phase of the switch breakdown.

To check this point more precisely, the paschen curve for this switch is plotted in Figure 5. Based on the experimental data points an expression such as

$$V_1 = 1.6 (pd)^{\frac{1}{2}} + 18.9 (pd) \quad (12)$$

was deduced to fit the experimental results fairly

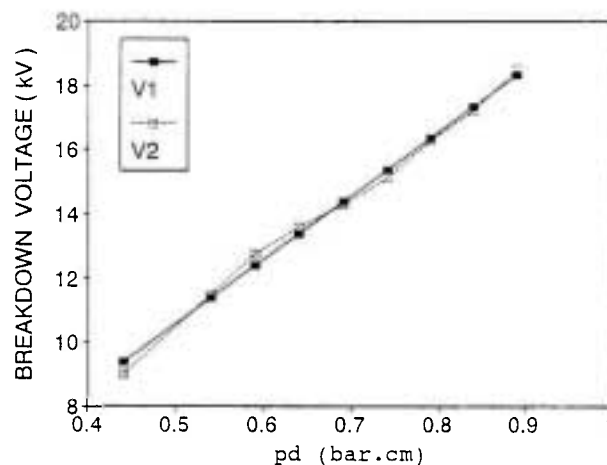


**Figure 5.** Variation of the measured average breakdown voltage,  $V_2$ , with respect to  $(pd)$  product for the gap. The values of  $V_1$  are based on the introduced Equation 12.

well. The curve based on Equation 12 is also displayed in Figure 5 which shows a good agreement between the two plots. If Equation 12 is compared with Equation 10 for the breakdown voltages in the air, several interesting results will be obtained. First, both equations, in general, show a similar  $(pd)$  dependence. Second, there are obvious differences in the constant values of  $E_c$  and  $K/C$  as expected. Comparing the critical ionization field,  $E_c$ , it can be observed that because of the presence of the trigger electrode, the effective ionization starts at a relatively lower value of the applied field (18.9 kV/cm). Because of the trigger pin, secondary processes in comparison to the self breakdown condition are enhanced which result in a higher value for the secondary ionization coefficient  $\gamma$ . This fact can be deduced from a decrease in the value of  $K$  in Equation 12, and the point that there is an inverse relation between  $K$  and  $\gamma$ , Equation. 4.

On the other hand, for the mesh electrode a similar relation can be developed, but the best expression has proved to be

$$V_1 = 3.4 (pd)^{\frac{1}{2}} + 3.3 (pd) + 0.7 (pd)^2 \quad (13)$$

where Equation 13 has an extra dependence on  $(pd)^2$

as well. For a small value of (pd), this term has a little contribution to the voltage breakdown, but as (pd) increases, its effect also increases considerably. The measured average breakdown voltages and calculated values from Equation 13 are presented in Figure 6.

Considering Equation 13, it can be concluded that the breakdown field in this case is not uniform and the mesh electrode has distorted the applied field considerably. This fact can be checked by comparing this breakdown voltage with that of self-breakdown voltage. By comparing Equations 13 and 10, which are both for the air, it is found that the  $E_c$  is considerably decreased, and also  $K/C$  shows a decrease from the value of 45.16 to 13.69 (kV)<sup>2</sup>/cm. This result indicates that the secondary effects have changed the breakdown field pattern irregularly in the case of the mesh triggering electrode.

As was stated in our recent report [15], the pressure controlled spark gap with cathode-mounted pin electrode gave a better performance in terms of regular firing and stability. The output power of the nitrogen laser for the case in which triggering, was accomplished by the pressure-controlled spark gap was almost twice the case of the other spark gap

switch. But at that time we did not have a clear answer for this effect. The result of this study clearly shows the reason for this difference, which is directly related to the breakdown conditions for the switches. The better performance of the pressure controlled spark gap is due to the fact that the field distortion caused by the third electrode is nearly uniform in this spark gap whereas the other breakdown discharge is nonuniform.

In summary the results of this study can be summarized as follows: (1) for externally triggered-electrodes, the gap breakdown voltage is considerably lower than the self-breakdown voltage; (2) the field distortion greatly depends upon the trigger electrode geometry and its place inside the discharge region; (3) Empirical expression for the breakdown voltage of each gap is obtained. The behavior of the breakdown voltage for the pressure controlled spark gap with a trigger electrode inside the cathode is nearly similar to that of the uniform field breakdown voltage; and (4) Because of the uniformity in its discharge, the pressure-controlled spark gap gives a better performance in terms of regular firing, stability, and as a result higher output power, when employed in a nitrogen laser as the trigger element.

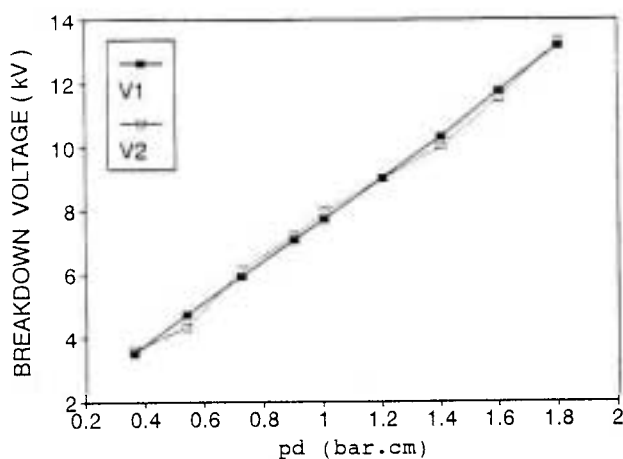


**Figure 6.** Variation of the measured average breakdown voltage,  $V_2$ , Versus (pd) product for the gap (a). The values of  $V_1$  are calculated from introduced Equation 13.

## REFERENCES

1. I. Santa, L. Kozma, B. Racz, and M. R. Gorbal, "High-Stability Thyatron-switched TEA Nitrogen Laser," *J. Phys. E: Sci. Instrum.*, Vol. 17, (1984) 368-370.
2. R. J. Rout, "Triggered Spark Gaps for Image Tube Pulsing," *J. phys. E: Sci. Instrum.*, Vol. 2, (1969) 739.
3. V. Hasson and H. M. Von Bergmann, "High Pressure Glow Discharges for Nanosecond Excitation of Gas Lasers and Low Inductance Switching Application," *J. Phys. E: Sci. Instrum.* vol. 9, (1976) 243-247.
4. H. M. Von Bergamann, "High Speed Multichannel Surface Spark Gaps," *J. Phys. E: Sci. Instrum.*, Vol. 15,

- (1981) 243-247.
5. J. W. Keto, T. D. Raymond and S. T. Walsh, "Low Inductance Spark Gap Switch for Blumlein-driven Lasers," *Rev. Sci. Instrum.*, Vol. 51, (1980) 42-43.
  6. J. M. Buzzi, H. J. Doucet, W. D. Jones, H. Lamain and C. Rouille, "A Very-low-inductance Triggered Multi-channel Surface Switch," *Rev. Sci. Instrum.*, Vol. 61, (1990) 852-858.
  7. T. Y. Tou, K. S. Low and B. C. Tan, "A Simple Two Stage Cascading Spark Gap for Ultraviolet Preionized Transversely Excited Atmospheric Co<sub>2</sub> Lasers," *Rev. Sci. Instrum.*, Vol. 62, (1991) 2584-2587.
  8. H. Golnabi, "Reliable Spark Gap Switch for Laser Triggering," *Rev. Sci. Instrum.*, Vol. 63, (1992) 5804-5805.
  9. H. Golnabi, "Nitrogen Laser Charging Process Investigation," *IEEE J. Quantum Electron.*, QE-29, (1993) 1192-1198.
  10. G. Parker, "A Novel Triggered Spark Gap for a High-Power xenon Flash," *Rev. Sci. Instrum.*, Vol. 60, (1989), 3337-3339.
  11. E. Nasser, "Fundamental of Gaseous Ionization and Plasma Electronics", Wiley-Interscience, (1971).
  12. J. S. Townsend, "Electricity in Gases," Oxford, (1914).
  13. E. Kuffel and W. S. Zaengl, "High-voltage Engineering Fundamentals," Oxford: Pergamon Press, Ch. 5 (1984).
  14. J. M. Meek and J. D. Craggs. "Electrical Breakdown of Gases," : Wiley, Ch. 7 (1978).
  15. H. Golnabi and H. Samimi, "Triggerable Spark Gap Switches for Pulsed Gas Lasers," *Rev. Sci. Instrum.*, Vol. 65, (1994) 3030-3031.